

## Flexible, weavable and efficient microsupercapacitor wires based on polyaniline composite fibers incorporated with aligned carbon nanotubes†

Cite this: *J. Mater. Chem. A*, 2013, **1**, 258

Zhenbo Cai,<sup>a</sup> Li Li,<sup>ab</sup> Jing Ren,<sup>a</sup> Longbin Qiu,<sup>a</sup> Huijuan Lin<sup>a</sup> and Huisheng Peng<sup>\*a</sup>

Received 12th September 2012  
Accepted 23rd October 2012

DOI: 10.1039/c2ta00274d

[www.rsc.org/MaterialsA](http://www.rsc.org/MaterialsA)

A supercapacitor in a flexible wire format has potential advantages that are described in this paper. Polyaniline composite fibers incorporated with aligned multi-walled carbon nanotubes are first synthesized with high mechanical strength and electrical conductivity through an easy electrodeposition process, and two robust composite fibers have then been twisted to produce microsupercapacitor wires with a specific capacitance of 274 F g<sup>-1</sup> or 263 mF cm<sup>-1</sup>. These energy storage wires are light-weight, flexible, strong and weavable for promising applications in various fields.

### Introduction

Supercapacitors have been generally fabricated in a rigid plate which is unfavorable for many applications, *e.g.*, portable and highly integrated equipment which needs to be small size, light-weight, and highly flexible.<sup>1–4</sup> As a result, flexible devices have recently become the subject of active research as a good solution.<sup>1,5,6</sup> A lot of effort has been dedicated to achieve these goals mainly by developing flexible planar supercapacitors, while wire-shaped supercapacitors are rare.<sup>5–8</sup> However, compared with the conventional planar structure, a supercapacitor wire which is weavable may exhibit unique and promising applications.<sup>9,10</sup> This fact may be explained by the much stricter requirement for the electrode such as a combined elaborate surface, high flexibility and remarkable electrochemical activity in wire-shaped supercapacitors.

On the other hand, conducting polymers such as polyaniline (PANI) are widely studied for electrode materials in electrochemical supercapacitors due to their high electrical conductivity and pseudo capacitance.<sup>11–16</sup> Unfortunately, PANI shows an obvious volume change during the charge and discharge process, which has largely decreased its mechanical stability during use. Carbon nanotubes (CNTs) have been explored for their high surface area and remarkable mechanical, electrical and thermal properties, and are then incorporated into PANI to enhance the performance of supercapacitors.<sup>11,16</sup> However, the degrees of improvement were far from expected as the CNTs

had been randomly aggregated in the composite electrode by a typical solution process, and charges had to cross a lot of boundaries in random CNT networks with low efficiency.<sup>17–20</sup> To this end, the alignment of CNTs may provide an effective route to solve the above problem and improve the capacitive performance of composite electrodes.

Herein, we have developed a new family of polyaniline composite fibers incorporated with aligned multi-walled carbon nanotubes (MWCNTs). Two composite fibers are twisted to produce novel microsupercapacitor wires with a surprisingly high specific capacitance of 274 F g<sup>-1</sup> or 263 mF cm<sup>-1</sup> (Fig. 1). Due to their high flexibility, these microsupercapacitor wires can be easily woven into clothes, packages or other portable devices by conventional textile technology, and serve as self-powered electric generators.

### Experimental section

PANI was coated onto aligned MWCNT fiber electrodes through an electrochemical analyzer system (CHI 660D) using platinum

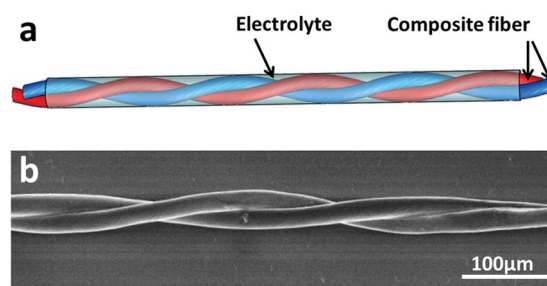


**Fig. 1** Two aligned MWCNT–PANI composite fibers twisted into a supercapacitor wire. (a) Schematic illustration. (b) Typical scanning electron microscopy (SEM) image.

<sup>a</sup>State Key Laboratory of Molecular Engineering of Polymers, Department of Macromolecular Science and Laboratory of Advanced Materials, Fudan University, Shanghai 200438, China. E-mail: penghs@fudan.edu.cn

<sup>b</sup>College of Food Science and Technology, Shanghai Ocean University, Shanghai 201306, China

† Electronic supplementary information (ESI) available. See DOI: 10.1039/c2ta00274d

wire and Ag/AgCl as counter and reference electrodes, respectively. Bare MWCNT fibers were first dipped into the electrolyte containing 1 M H<sub>2</sub>SO<sub>4</sub> and 0.1 M aniline for 5 h, so the aniline monomer can be effectively infiltrated into them. Electropolymerization of aniline was mainly performed from 50 to 2000 s at a potential of 0.75 V. After polymerization, the as-prepared MWCNT–PANI composite fibers were washed with deionized water and dried at room temperature for over 2 h. The aligned MWCNT–PANI composite fibers were then coated with a layer of gel electrolyte containing 10 wt% poly(vinyl alcohol) and 2.5 wt% H<sub>3</sub>PO<sub>4</sub> on the surface (Fig. S1†). Two modified composite fibers were finally twisted to fabricate the supercapacitor wire. The electrochemical measurements of supercapacitor wires were performed using an ARBIN multi-channel electro-chemical testing system.

The structures of aligned MWCNT–PANI composite fibers were characterized by transmission electron microscopy (TEM, JEOL JEM-2100F operated at 200 kV), scanning electron microscopy (SEM, Hitachi FE-SEM S-4800 operated at 1 kV), Raman spectroscopy (Renishaw inVia Reflex with an excitation wavelength of 514.5 nm and laser power of 20 mW) and Fourier transform infrared spectroscopy (ThermoFisher Nicolet 6700). Galvanostatic charge–discharge measurements of supercapacitor wires were taken at a current density of 2 A g<sup>−1</sup>. The specific resistances were measured by an alternating current complex impedance method. The average specific capacitance of the electrode derived from the galvanostatic discharging curve was calculated according to the following equation:  $C = 2i_0/[m(\Delta V/\Delta t)]$ , where  $i_0$ ,  $\Delta V/\Delta t$  and  $m$  correspond to the discharge current, average slope of the discharge curve and mass of the active MWCNT–PANI material in the electrode, respectively. Here the mass of PANI was calculated from the total depositing charge in the cathode with 2.5 electrons per aniline monomer in emeraldine.

## Results and discussion

MWCNT fibers were first spun from spinnable MWCNT arrays which were typically synthesized by chemical vapor deposition. The synthesis of spinnable MWCNT arrays was reported elsewhere,<sup>21,22</sup> and the diameter of MWCNTs was about 10 nm. The resulting MWCNT fibers had been controlled from about 10 to 20 μm in diameter and up to hundreds of meters in length. Fig. 2a shows a scanning electron microscopy (SEM) image of a typical MWCNT fiber with uniform diameter of 15 μm, which has been mainly studied in this work. Fig. 2b further exhibits that MWCNTs are highly aligned in the fiber at a higher magnification, which has been shown to enable excellent mechanical and electrical properties, e.g., tensile strengths of 10<sup>2</sup> to 10<sup>3</sup> MPa and electrical conductivities of 10<sup>3</sup> S cm<sup>−1</sup>. A lot of voids existed among aligned MWCNTs typically with sizes of tens of nanometers, and a second phase, such as conducting polymers, could then be easily electrodeposited onto the MWCNTs and infiltrated into the voids.

Electrochemical deposition of PANI was made on aligned MWCNT fiber electrodes through an electrochemical analyzer system using platinum wire and Ag/AgCl as counter and

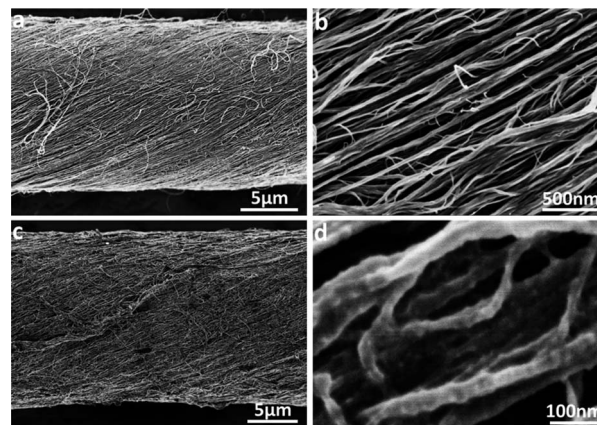


**Fig. 2** SEM images of (a and b) bare aligned MWCNTs and (c and d) MWCNT–PANI composite fibers with a PANI weight percentage of 34% at different magnifications.

reference electrodes, respectively. After introduction of PANI, the resulting MWCNT–PANI composite fiber remained almost unchanged in diameter. Fig. 2c shows a typical SEM image of the composite fiber with a diameter of 15 μm, which was the same as the bare MWCNT fiber. Fig. 2d, S2 and S3† show that the MWCNTs remained highly aligned after electrodeposition, and PANI had been uniformly coated onto the MWCNTs in the composite fiber. The voids among MWCNTs were found to be filled with PANI at a weight percentage of 40%. With the further increase of PANI, the additional polymer was mainly coated on the outer surface of fibers. Fig. S4† shows typical SEM images of composite fibers with a weight percentage of 70%, and the additional PANI was coated on the fiber surface.

The resulting MWCNT–PANI composite fibers were flexible and could be easily bent. No obvious damage to the structure was observed under SEM, and both tensile strength and electrical conductivity remained almost unchanged after bending for over a hundred cycles. PANI could be stably attached on the aligned MWCNTs possibly due to the interaction between them in the composite fiber. Fig. S5 and S6† have compared the Raman spectra and Fourier transform infrared spectra of PANI, MWCNT and MWCNT–PANI composite fiber with PANI weight percentage of 24%. The peaks at 1618 cm<sup>−1</sup> for the C–C stretch of benzenoid ring and 1193 cm<sup>−1</sup> for the C–H stretch of quinoid ring in the pure PANI shifted to 1616 and 1185 cm<sup>−1</sup> in the aligned MWCNT–PANI composite fiber, respectively, which indicated the  $\pi$ – $\pi$  interaction between aligned MWCNT and PANI.<sup>23–25</sup> The wavelength and intensity ratio of D and G bands have also been often used to study the interaction between MWCNT and other incorporated components.<sup>26,27</sup> Here both D and G bands are overlapped with the peaks of PANI, so it is difficult to directly compare them before and after formation of the composite fibers.

Compared with bare MWCNT fibers, the polymer chains bundled the neighboring MWCNTs more closely to decrease the slide and reduce the contact resistance among MWCNTs.<sup>28,29</sup> The bundling effect was further strengthened by the  $\pi$ – $\pi$  interaction between MWCNT and PANI.<sup>28</sup> Accordingly, the

resulting composite fiber showed a higher tensile strength than the bare fiber. As shown in Fig. S7,<sup>†</sup> the strength of a composite fiber with a PANI weight percentage of 34% has been improved by 58%. The electrical conductivity remained almost the same after formation of composite fibers.

The aligned MWCNT–PANI composite fibers were then coated with a layer of  $\text{H}_3\text{PO}_4$ –poly(vinyl alcohol) gel electrolyte on the surface. Two modified composite fibers were finally twisted to fabricate the supercapacitor wire. Cyclic voltammetry was first used to characterize the electrochemical properties of bare aligned MWCNT and MWCNT–PANI composite fibers. Fig. 3a has compared the cyclic voltammograms (CVs) of a MWCNT and MWCNT–PANI composite fiber with a PANI weight percentage of 24% measured in a two-electrode system at a scan rate of  $10 \text{ mV s}^{-1}$ . Obviously, a typical rectangular shape which corresponds to a double layer capacitor is obtained for the bare MWCNT fiber, while redox peaks at 0.3–0.4 V that indicate a pseudo-capacitance derived from different oxidation states of PANI are observed for the MWCNT–PANI composite fiber. As expected, the current density for the composite fiber is much higher than that of the bare MWCNT fiber. Fig. 3b shows typical Galvanostatic charge–discharge curves of the composite fiber electrode between 0 and 0.8 V at a current density of  $2 \text{ A g}^{-1}$ . It can be found that the charge curves are nearly symmetrical to their corresponding discharge curves in the potential range,

which indicates a high reversibility between charge and discharge processes.

The supercapacitor wire also showed a high stability during use. Fig. 3c shows the dependence of specific capacitance on the cycle number. It was slightly decreased in the first 50 cycles and then remained unchanged in the following 950 cycles. Fig. 3c also shows that the Coulomb efficiency maintained 99% over 1000 cycles. The specific capacitances increase with the increasing PANI weight percentage (Fig. 3d). For instance, the specific capacitances are improved from 4.5, 78, 114, 177 to  $274 \text{ F g}^{-1}$  with the increasing PANI weight percentage from 0, 7.4, 19, 29, to 48% at a current density of  $2 \text{ A g}^{-1}$ , respectively. The increasing specific capacitance with the PANI weight percentage is mainly derived from the higher pseudocapacitance provided by the deposited PANI. Interestingly, further increase of PANI has decreased the specific capacitance, e.g.,  $245 \text{ F g}^{-1}$  at 70 wt%,

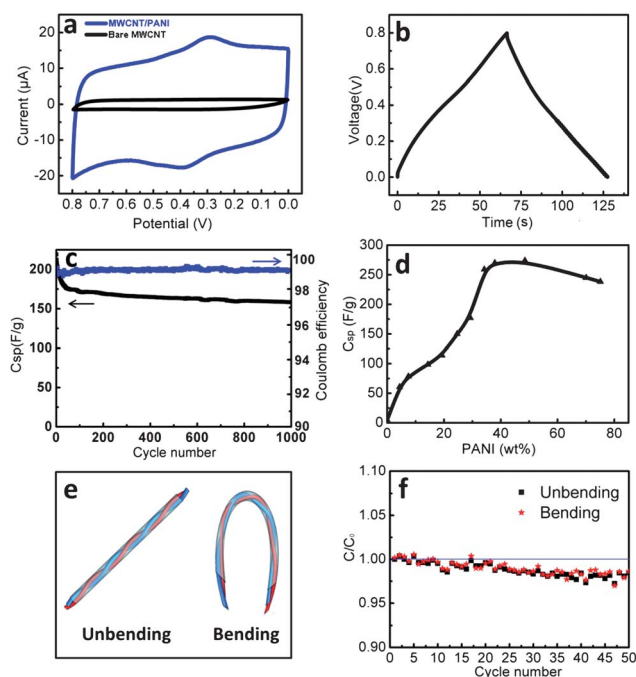


**Fig. 3** Electrochemical properties of supercapacitor wires. (a) Cyclic voltammogram of a supercapacitor based on a PANI weight percentage of 24%. (b) Galvanostatic charge–discharge curves of a supercapacitor based on a PANI weight percentage of 24%. (c) Dependence of specific capacitance and Coulomb efficiency on cycle number of a supercapacitor based on a PANI weight percentage of 34%. (d) Dependence of specific capacitance on the PANI weight percentage. (e) Schematic illustration of the unbending and bending morphologies. (f) Dependence of the specific capacitance of a supercapacitor based on a PANI weight percentage of 34% on bending cycle number.  $C_0$  and  $C$  correspond to the specific capacitance before and after bending.

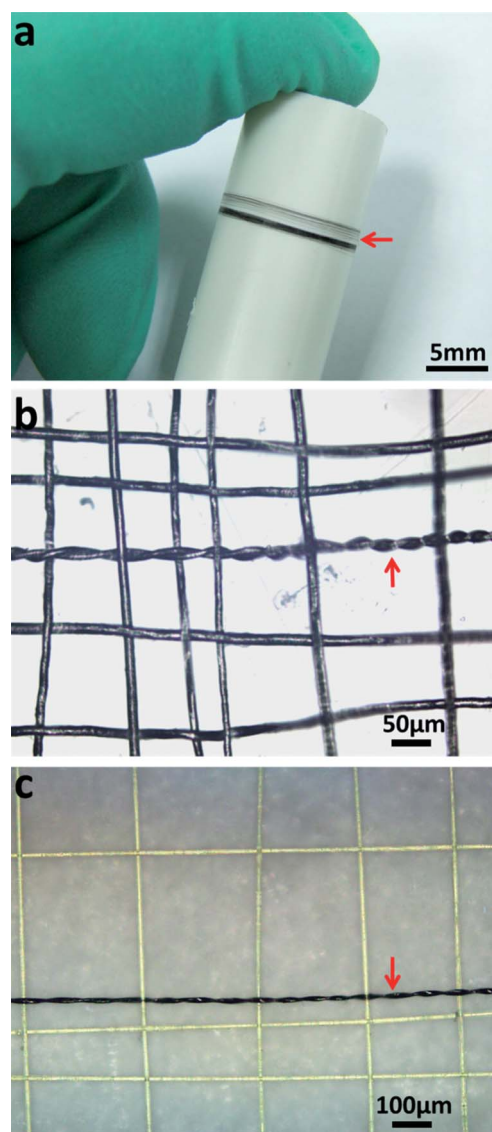


**Fig. 4** The supercapacitor wire woven into textile structures. (a) A continuous and long wire. (b) Woven with the other CNT fibers. (c) Woven into a textile composed of aramid fibers. The red arrows show the wire.

which may be explained by a different structure in the composite fiber with the increasing PANI weight percentage. PANI was mainly deposited on the outer surfaces of individual MWCNTs at a weight percentage of lower than 40%, where excellent electrical properties such as high conductivity were observed. With further electrodeposition at a higher percentage, the additional PANI would cover the outer surface of the MWCNT fiber, thereby not taking advantage of the aligned structure of the MWCNTs. In fact, pristine PANI on a flexible indium tin oxide substrate showed a low specific capacitance of  $10.2 \text{ F g}^{-1}$ .

The supercapacitors were also flexible and can be bent without an obvious decrease in structure stability traced by SEM. The flexibility and stability were further characterized by measuring the galvanostatic charge–discharge curves under different bending cycles (Fig. 3e). Fig. 3f shows the dependence of  $C/C_0$  for a supercapacitor wire fabricated from a MWCNT–PANI composite fiber (with a PANI weight percentage of 70%) with an increasing number of bending cycles. Here  $C_0$  and  $C$  correspond to the specific capacitances before and after bending. The values of  $C/C_0$  only slightly decrease by less than 3% after 50 cycles of bending.

As the MWCNT fiber had been continuously spun from arrays, the supercapacitor wire could also be scaled up for practical applications (Fig. 4a). In addition, due to the high flexibility, the supercapacitor wires were easily woven into different textiles. Fig. 4b and c show that they could be woven with each other or woven into chemical fibers such as a poly(*p*-phenylene terephthalamide) textile. The light-weight and high strength of such supercapacitor wires also provides them with unique and promising applications.

## Conclusions

In summary, highly aligned MWCNT–PANI composite fibers were continuously synthesized with excellent mechanical, electrical, and electrochemical properties through an easy electrodeposition process. They were further twisted to fabricate novel wire-shaped supercapacitors with high specific capacitances up to  $263 \text{ mF cm}^{-1}$ . The light-weight, high flexibility, high strength, and good weavability provide them with promising applications in various fields. This work also presents a fabrication paradigm for the development of high performance energy storage devices based on the use of new electrode nanomaterials.

## Acknowledgements

This work was supported by NSFC (20904006, 91027025), MOST (2011CB932503, 2011DFA51330), MOE (NCET-09-0318), STCSM (11520701400), CPSF (2011M500724), The Program for Professor of Special Appointment (Eastern Scholar) at Shanghai Institutions of Higher Learning and State Key Laboratory of Molecular Engineering of Polymers at Fudan University (K2011-10).

## Notes and references

1 M. Kaempgen, C. K. Chan, J. Ma, Y. Cui and G. Gruner, *Nano Lett.*, 2009, **9**, 1872–1876.

- 2 C. Meng, C. Liu and S. Fan, *Electrochem. Commun.*, 2009, **11**, 186–189.
- 3 J. Liu, J. Sun and L. Gao, *J. Phys. Chem. C*, 2010, **114**, 19614–19620.
- 4 Z. Niu, P. Luan, Q. Shao, H. Dong, J. Li, J. Chen, D. Zhao, L. Cai, W. Zhou, X. Chen and S. Xie, *Energy Environ. Sci.*, 2012, **5**, 8726–8733.
- 5 J. Bae, M. K. Song, Y. J. Park, J. M. Kim, M. Liu and Z. L. Wang, *Angew. Chem., Int. Ed.*, 2011, **50**, 1683–1687.
- 6 J. A. Lee, M. K. Shin, S. H. Kim, S. J. Kim, G. M. Spinks, G. G. Wallace, R. Ovalle-Robles, M. D. Lima, M. E. Kozlov and R. H. Baughman, *ACS Nano*, 2011, **6**, 327–334.
- 7 P. Chen, H. Chen, J. Qiu and C. Zhou, *Nano Res.*, 2010, **3**, 594–603.
- 8 A. B. Dalton, S. Collins, E. Muñoz, J. M. Razal, V. H. Ebron, J. P. Ferraris, J. N. Coleman, B. G. Kim and R. H. Baughman, *Nature*, 2003, **423**, 703.
- 9 T. Chen, L. Qiu, H. G. Kia, Z. Yang and H. Peng, *Adv. Mater.*, 2012, **24**, 4623–4628.
- 10 T. Chen, L. Qiu, Z. Cai, F. Gong, Z. Yang, Z. Wang and H. Peng, *Nano Lett.*, 2012, **12**, 2568–2572.
- 11 C. Meng, C. Liu, L. Chen, C. Hu and S. Fan, *Nano Lett.*, 2010, **10**, 4025–4031.
- 12 Q. Wu, Y. Xu, Z. Yao, A. Liu and G. Shi, *ACS Nano*, 2010, **4**, 1963–1970.
- 13 L. Nyholm, G. Nyström, A. Mihranyan and M. Strømme, *Adv. Mater.*, 2011, **23**, 3751–3769.
- 14 B. Ding, X. Lu, C. Yuan, S. Yang, Y. Han, X. Zhang and Q. Che, *Electrochim. Acta*, 2012, **62**, 132–139.
- 15 C. Li, H. Bai and G. Shi, *Chem. Soc. Rev.*, 2009, **38**, 2397–2409.
- 16 G. Wang, L. Zhang and J. Zhang, *Chem. Soc. Rev.*, 2012, **41**, 797–828.
- 17 H. Lee, H. Kim, M. S. Cho, J. Choi and Y. Lee, *Electrochim. Acta*, 2011, **56**, 7460–7466.
- 18 X. Lu, H. Dou, C. Yuan, S. Yang, L. Hao, F. Zhang, L. Shen, L. Zhang and X. Zhang, *J. Power Sources*, 2012, **197**, 319–324.
- 19 F. Huang, E. Vanhaecke and D. Chen, *Catal. Today*, 2010, **150**, 71–76.
- 20 H. Zhang, G. Cao and Y. Yang, *Energy Environ. Sci.*, 2009, **2**, 932–943.
- 21 Q. W. Li, X. F. Zhang, R. F. DePaula, L. X. Zheng, Y. H. Zhao, L. Stan, T. G. Holesinger, P. N. Arendt, D. E. Peterson and Y. T. Zhu, *Adv. Mater.*, 2006, **18**, 3160–3163.
- 22 J. Zhao, X. Zhang, J. Di, G. Xu, X. Yang, X. Liu, Z. Yong, M. Chen and Q. Li, *Small*, 2010, **6**, 2612–2617.
- 23 L. Li, Z.-Y. Qin, X. Liang, Q.-Q. Fan, Y.-Q. Lu, W.-H. Wu and M.-F. Zhu, *J. Phys. Chem. C*, 2009, **113**, 5502–5507.
- 24 H. Fan, H. Wang, N. Zhao, X. Zhang and J. Xu, *J. Mater. Chem.*, 2012, **22**, 2774–2780.
- 25 T.-M. Wu, Y.-W. Lin and C.-S. Liao, *Carbon*, 2005, **43**, 734–740.
- 26 T. Chen, S. Wang, Z. Yang, Q. Feng, X. Sun, L. Li, Z.-S. Wang and H. Peng, *Angew. Chem., Int. Ed.*, 2011, **50**, 1815–1819.
- 27 W. Wang, X. Sun, W. Wu, H. Peng and Y. Yu, *Angew. Chem.*, 2012, **124**, 4722–4725.
- 28 H. Peng, X. Sun, F. Cai, X. Chen, Y. Zhu, G. Liao, D. Chen, Q. Li, Y. Lu, Y. Zhu and Q. Jia, *Nat. Nanotechnol.*, 2009, **4**, 738–741.
- 29 W. Guo, C. Liu, X. Sun, Z. Yang, H. G. Kia and H. Peng, *J. Mater. Chem.*, 2012, **22**, 903–908.